

## Sulfide Stabilization in Geothermal Applications

Duygu Disci, Argyro Spinthaki and Hande Sile

Kurita Europa GmbH, Mannheim, Germany

duygu.disci@kurita-water.com

**Keywords:** geothermal, scale, precipitation, sulfide, antimony, lead, energy, inhibition

### ABSTRACT

Scale formation is commonly observed in geothermal power plants due to high salt content, high temperatures, and varying pH conditions altering the solubility of salts. Scaling at surface facilities impairs the heat transfer, reduces the overall plant efficiency, which limits the total power output, and in severe cases leads to equipment losses as well. Despite the common scale types of carbonates and silicates, deposition of sulfides is considerably encountered. This type of deposition is especially observed in binary cycle geothermal power plants. Among various sulfide scales including arsenic and iron, the focus of this contribution will be antimony and lead-rich sulfide scales in geothermal utilization. Sulfide scale formation is more geographically dependent regarding the characteristics of the reservoir. Studying the geothermal plants worldwide, antimony sulfide precipitation is mainly reported on the west coast of Turkey, in Italy and in New Zealand, whereas lead sulfide is mainly reported in Japan, North-West Turkey, Upper Rhine Graben and Greece. Despite the widely conducted research on carbonate and silicate scaling, studies concerning the mitigation strategies toward sulfides are limited. This contribution will present the effect of successful stabilizers for antimony sulfide and lead sulfide mainly dedicated to geothermal applications. Laboratory studies will be shown for both deposit types, and a case study for antimony sulfide stabilization will be demonstrated with physical parameters observed during the treatment program in the field.

### 1. INTRODUCTION

The increase of energy production based on geothermal sources during the last years is remarkable. (Shortall and Uihlein, 2019). The reason for the increase in this alternative energy utilization is the numerous attractive characteristics and multiple matches to the list of Sustainability Targets. Salton Sea geothermal brines in South Eastern California and geothermal brines beneath the Cheleken Peninsula on the Caspian Sea are, amongst others, two of the most common and modern examples of mineral-rich hydrothermal systems. Geothermal brines are aqueous solutions containing a variety of different ions: primarily sodium, potassium, calcium, silica (either as colloidal or silicate), aluminum, zinc, antimony, lead, sulfide and chloride (Bucher and Stober, 2010). In addition, they may also contain significant amounts of other alkali metals, alkaline-earth metals, transition metals, and halides (White, 1981). Expectedly, scale deposits that form in geothermal brines vary considerably in composition, depending on the geographical location and their respective surrounding environments. Processes such as the decrease of temperature, condensation or dilution, increase of pH, reaction with sulfides and redox reactions can easily be the cause of precipitation of minerals and other scales from geothermal fluids (Gallup, 1998a). Scaling processes and deposition are notorious for generating challenging operational conditions and / followed by catastrophic failures in plant operation for geothermal systems, thus different scale types have been under the scientific microscope for many decades. The focus of this work is on sulfide scales, which are frequently encountered in geothermal operations and have been observed in high temperature as well as in low/medium temperature resources. They are commonly associated with other metal cations, forming scale deposits that are very tenacious and difficult to handle. In contrast to many other scales such as silicates, many metal sulfides, as they occur in geothermal brines, are well – characterized crystalline mineral salts with low solubility constants ( $K_{sp}$ ) (Smith and Martel, 1976).  $S^{2-}$  species are dominant at  $pH > 11$ , while at circumneutral pH,  $HS^-$  is found at higher

concentrations. Several heavy metal sulfides are found in scale deposits formed by the flow of high-enthalpy and high-salinity geothermal brines.

### 1.1 Lead Sulfide

In general, lead sulfide is the most likely to appear of the metal sulfides family in high total dissolved solids / high enthalpy fluids due to the abundance of its respective components and its low solubility constant. Studies reported in literature provide information on several behavioral characteristics, such as the scale's deposition rate obtained in once-through experiments. Such studies lead to the identification of the mechanism causing lead sulfide scaling (Andritsos and Karabelas, 1991a). The procedure of lead sulfide formation and precipitation is highly pH dependent but can also be influenced from other brine and operational characteristics such as flow rate, temperature and ionic strength (salinity). Lead sulfide solubility has been reported to experience a minimum at pH 7, similar to other members of the metal sulfide family, namely Fe and Zn sulfides (Andritsos and Karabelas, 1995). Crucially for geothermal – based operations, temperature and salinity have been reported to shift the minimum solubility pH to higher values (Andritsos and Karabelas, 1991b). These factors also affect the morphology and growth rate of lead sulfide deposits. Specifically, the particle size of lead sulfide deposits has been reported to increase at low supersaturation conditions and vice versa (Andritsos and Karabelas, 1991a).

### 1.2 Antimony Sulfide

Antimony (III) sulfide scaling, commonly known as stibnite, is considered highly problematic when it forms in geothermal systems, but its presence is limited geographically, and it is not a universal foulant. Examples of areas with antimony (III) sulfide presence include Western Turkey, Italy and New Zealand. The electron configuration of Sb is  $[Kr]4d105s25p3$ , and thus, it can possess two basic oxidation states: trivalent Sb(III), which forms  $Sb_2S_3$  with sulfides, and pentavalent Sb(V), which forms  $Sb_2S_5$  with sulfides. Antimony (III) Sulfide is found in two forms, crystalline (stibnite – gray, well-defined structure) and amorphous (metastibnite – red, non –stoichiometric). It is worth mentioning that stibnite is a very insoluble mineral salt that shows enhanced precipitation as pH and temperature increase and has a solubility constant ( $K_{sp}$ ) of about  $1.5 \times 10^{-93}$  (Smith and Martel, 1976).  $Sb_2S_5$  is poorly characterized and has not been unequivocally identified as a geothermal deposit. It is also widely known that sulfide is oxidized by oxygen and there may be an inherent redox chemistry causing complications. The problems mainly reported from geothermal plants is that this aggressive scale type is primarily depositing on the heat exchangers, where temperature fluctuation is major, leading to decrease of the scale solubility. This leads to decreased power production, decrease in the differential pressure and insufficient cooling heat exchange. Therefore, a chemical remedy is the required solution to avoid numerous mechanical cleanings of the system and thus frequent stand bys and high maintenance costs. Due to its low solubility constant, its inhibition has proven to be a challenging task. So far, a variety of different homo – and copolymers pose commercially as possible inhibitors, with the common feature of being highly anionic. In this work, we are headed towards an effective stabilizer that could prove useful in order to avoid the economical losses caused by this type of deposition. In general, the search for effective chemical additives in geothermal applications comes with a series of challenges and demands. Apart from its effectiveness against the targeted scaling or corrosion problems, the thermal stability of such a product is considered as a factor of the utmost importance, due to the high temperatures encountered in a geothermal plant. Furthermore, the ability of a product to be combined with further additives and to be affordable to be used on site is deemed crucial.

## 2. EXPERIMENTAL SECTION

### 2.1 Lead Sulfide

The test water is produced by dissolving the respective salts in de-ionized water (see Table 1). Lead sulfide was produced by adding aqueous solutions of lead acetate and sodium sulfide subsequently to the test water maintaining a stoichiometric ratio of 1:1.

**Table 1: Composition of test water and test conditions.**

Parameter	Unit	Value
Ca <sup>2+</sup>	mmol/L	160
Mg <sup>2+</sup>	mmol/L	0
Na <sup>+</sup>	ppm	25.000
Cl <sup>-</sup>	ppm	90.000
SO <sub>4</sub> <sup>2-</sup>	ppm	1.000
pH		6
Temperature	°C	25

For the scale inhibition effect evaluation, test water was mixed with 1 liter of DI water and the desired inhibitor amount in a glass beaker under a stirring speed of 300 rpm. For the dispersion approach, the inhibitor was added after a specified time frame of stirring to allow particle formation and growth. The results were evaluated in four ways.

Visual evaluation: the turbidity of the test solutions was judged visually, and photos taken. Turbidity: the turbidity of the test solutions was measured with an immersion probe VisoTurb 900-P from WTW, at a wavelength of 860 nm.

Particle size distribution: the size of the precipitated particles was evaluated using a LUMiSizer, an analytical centrifuge that measures the extinction of the transmitted light across the entire length of a sample (ISO 13318 - 2).

Analytical: the lead content was measured by plasma mass spectrometry (ICP-MS) after acidification of samples with nitric acid p.a. Table 2 summarizes the selected concentration of lead sulfide and inhibitor in the trials, as well as the evaluation methods used in each case.

**Table 2: Overview of methods used and key parameters for the evaluation of chemical additives against lead sulfide.**

Approach	Lead sulfide (mg/L)	Product conc. (mg/L)	Evaluation
Delay of growth of particles created in situ	15	50	Visual, Particle size distribution, Turbidity
Prevention of precipitation	3	100 – 500	Visual
Prevention of precipitation	1	10 – 500	Analysis of Pb

## 2.2 Antimony (III) Sulfide

In short, the laboratory tests are started with the preparation of the synthetic water as described in Table 3. The test water is produced by dissolving the respective salts in de-ionized water. Afterwards, the inhibitors are added and the images for the evaluation on the success of the inhibitor are obtained at defined time frames.

**Table 3: Composition of test water and test conditions.**

Parameters	Unit	Value
Test volume	mL	250
Duration	H	22
Temperature	°C	25
pH		7.5
CaH / MgH	ppm CaCO <sub>3</sub>	230 / 50
TAC	ppm CaCO <sub>3</sub>	185
Cl <sup>-</sup> / SO <sub>4</sub> <sup>2-</sup>	ppm	165 / 50
Antimony (III) Sulfide	ppm	20

### 3. RESULTS AND DISCUSSION

#### 3.1 Lead Sulfide

##### 3.1.1 Delay of particle growth – evaluation visually and by particle size measurement

Lead sulfide particles were produced under stirring for 3 minutes in presence of the inhibitor (dosed at the beginning of the trial). The working hypothesis is that an effective inhibitor reduces particle growth and thus the settling of the particles is slower, resulting in a longer lasting turbidity (Stokes' law).

Figure 1 shows beakers with a lead sulfide concentration of 15 mg/L, 6 hours after the stirring is stopped. The turbidity can be linked to the respective particle sizes measured at the end of the stirring time.

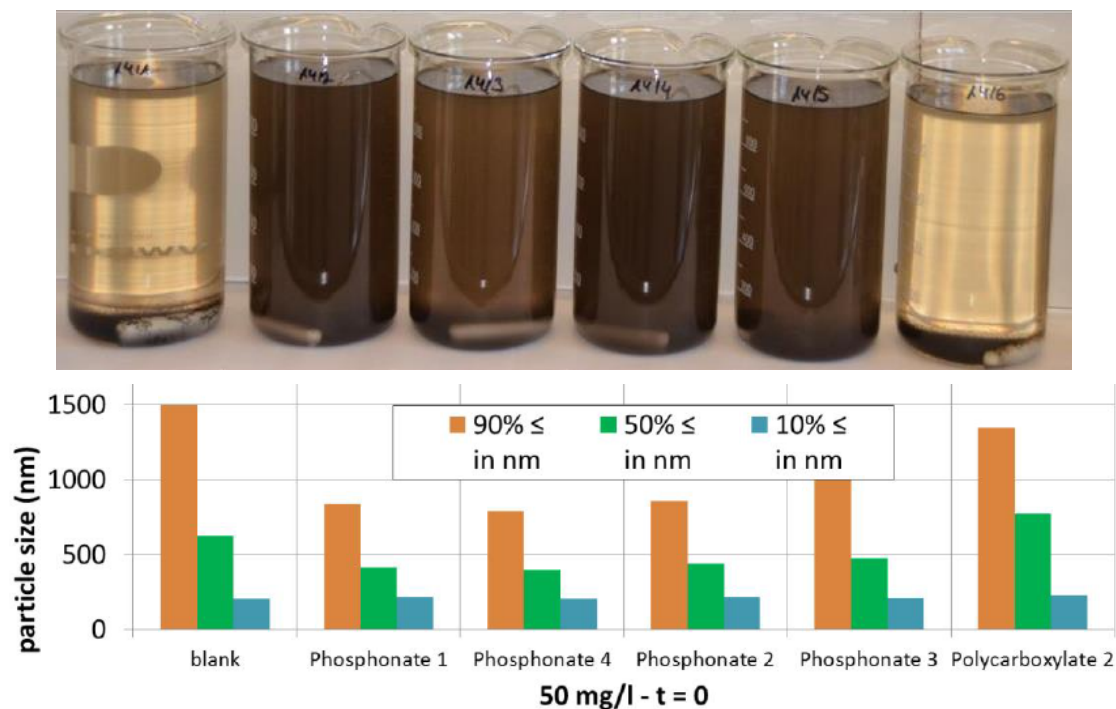


**Figure 1: Performance of inhibitors evaluated visually (6 hours settling time) and by particle size measurement directly after preparation.**

##### 3.1.2 Delay of particle growth – evaluation by turbidity

The observation that particle growth is enhanced with stirring time leads to an alternative evaluation method using a turbidity meter. With this approach, the stirring is continued over the entire trial time (1 h) and the resulting turbidity recorded.

The initial phase of these attempts are presented in Figure 2, where particles are best dispersed as long as they are small, followed by a phase of settlement caused by an increasing particle size (despite presence of inhibitor), arriving at a plateau that is maintained by rotation speed. The higher turbidity at the initiation of the experiment and the higher plateau after one hour can be attributed to smaller particle sizes respectively a good inhibitor performance.

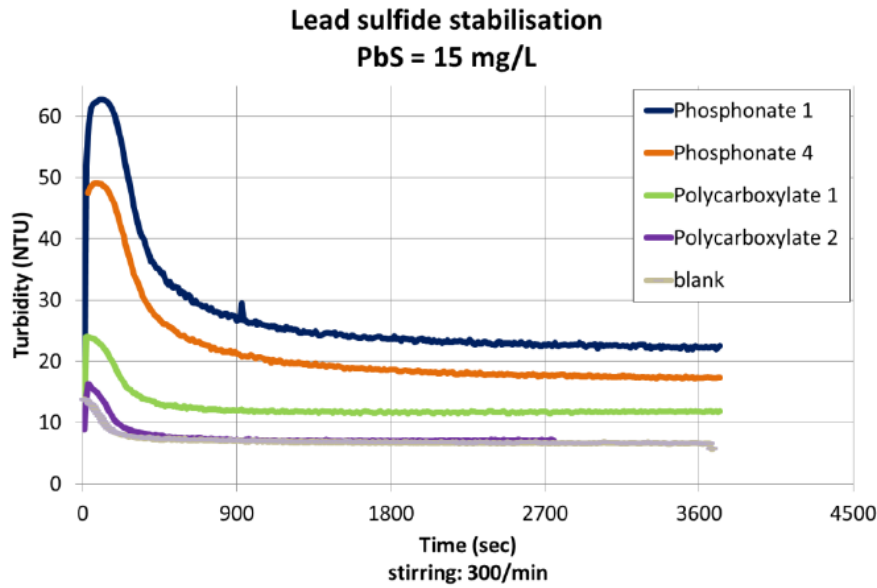


**Figure 2.** Turbidity of PbS suspension over time while stirring in dependence of different inhibitors dosed at 50 mg/L.

### 3.1.3 Prevention of precipitation

With 15 mg/L lead sulfide in the test water, inhibitor concentrations of 50 mg/L were only able to delay precipitations; for complete prevention it was found that concentrations > 1000 mg/L were necessary. In order to transfer this approach to lower thus more practical ranges, a lead sulfide concentration of 3 mg/L was set as the lowest possible limit for visual evaluation. By determining if a test solution stays clear (3), slightly turbid (2) or showed precipitation (1), a relative quick and easy distinction could be made regarding the inhibitor's capacities (see Figure 3).

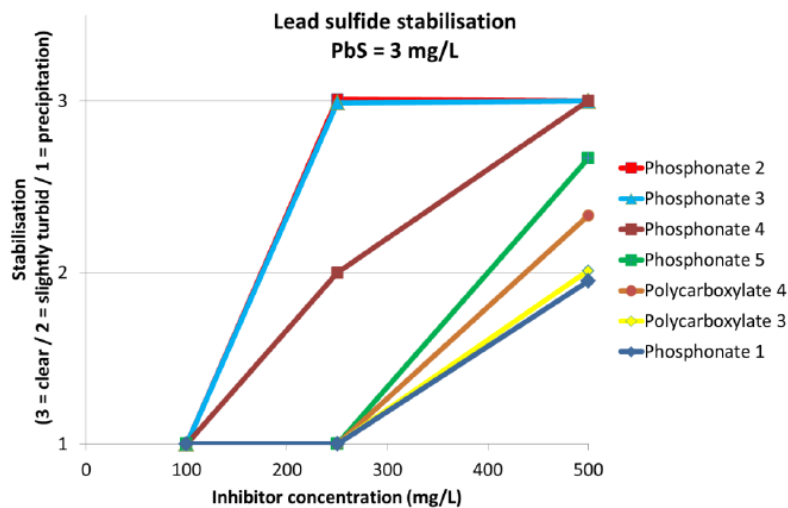


**Figure 3:** Prevention of lead sulfide scaling with different inhibitors and concentrations after 60 minutes.

### 3.1.4 Prevention of precipitation – evaluation by analysis

A lead sulfide concentration of 1 mg/L does no longer allow for a visual evaluation by eye. In order to substantiate the results as shown with the quick method (see Figure 4), the lead sulfide solution (1 mg/L) was filtered (0.45 µm) after stirring of 3 min and the lead content in the filtrate analyzed by ICP. This content divided by the calculated theoretical lead concentration of 867 µg/L yielded the relative stabilization (in percent). It is indicated that three representative inhibitors, that the ranking obtained matches the one found with the quick methods: phosphonate 2 > phosphonate 1 >> polycarboxylate 1 (the latter does

not appear in Figure 3 since it did not show any effect even at a concentration of 500 mg/L). While further testing at even lower lead sulfide concentrations than 1 mg/L would be desirable, the accuracy of this method would be increasingly compromised e.g. by adhesion effects (beaker, filter).

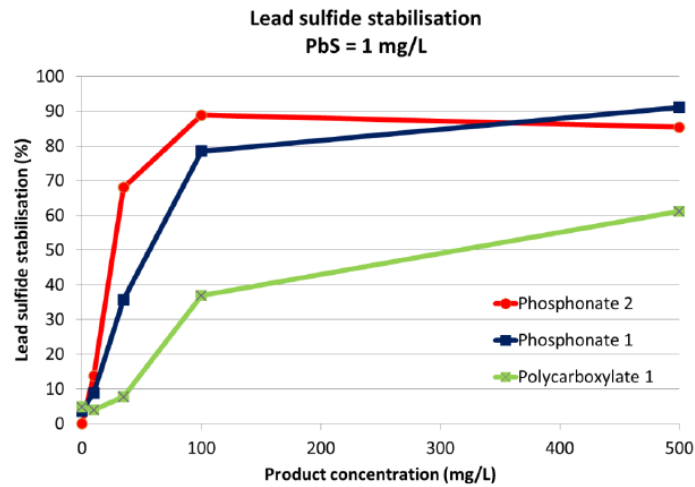


**Figure 4: Relative lead sulfide stabilization of different scale-inhibitors as function of inhibitor concentration.**

### 3.1.5 Dispersion

Similar to measuring stabilizing effects, the dispersing capability of inhibitors was tested. The key difference between stabilizing and dispersing experiments was the time when the additive was added: for the antiscalant tests the inhibitor to be evaluated was dosed at the beginning, for dispersing tests after 3 minutes of stirring when the scale precipitation had been practically finished. The best differentiation between the inhibitors respectively dispersants was eventually achieved under the following conditions (see also table 4): (a) limiting particle growth during the first 3 minutes with a good stabilizer: Phosphonate 1 was dosed at a concentration of 50 mg/L. (b) promoting particle agglomeration by another 12 minutes of stirring after dosing of dispersant. (c) evaluation of the suspension after 75 minutes of settling time.

**Table 4: key steps taken for the evaluation of dispersants for lead sulfide.**

Time (min)	Step
0	Start stirring Dosage of Phosphonate 1 (50 mg/L) Dosage of lead acetate and sodium sulfide (15 mg/L PbS)
3	Dosage of inhibitor/dispersant to be tested (50 mg/L)
15	Stop stirring
75	Evaluation



**Figure 5: Efficiency of lead sulfide dispersing of different inhibitors at 50 mg/l after 60 min of settling time (from left to right: blank, polycarboxylate 2, phosphonate 5, polycarboxylate 1, phosphonate 1, polycarboxylate 5).**

### 3.2 Antimony (III) Sulfide

A laboratory experimental set up was developed, where different chemistries were investigated as potential antimony sulfide inhibitors / dispersants. Successful lab trials lead to a field trial. In order to construct the laboratory set ups, three main properties were considered: reliability, differentiability and practical approach. The starting point was turbidity measurements; turbidity tests could be versatile however in this case the used concentration did not lead to a successful approach. In parallel to the turbidity measurements, the soluble sulfide concentration was measured; however, this approach needed to be as well dismissed. This is due to the fact that threshold inhibition seems to fail for Stibnite because of the very low solubility constant of this scale. In other words, left – over soluble sulfide in our experiments was negligible, meaning that the majority of the ionic moieties are precipitating as antimony sulfide.

Nevertheless, it is obvious that some of the selected candidates have a significant effect on the scale's morphology, mainly by affecting the crystal growth and particle size. Therefore, dispersion is mostly pursued as an effective anti-fouling approach. The visual observations during these tests turned out to be the easiest yet precise and differentiative evaluation approach. By modifying the test conditions, we developed our test strategy for Stibnite stabilization (see Figure 6). We tested a variety of different chemistries for this demanding task and proceeded to evaluate the results as seen in Figure 6. The four products, marked P1 to P4, are tested at 3 different concentrations for 22 hours. In the Control experiment we can monitor the precipitation of Stibnite as it proceeds in absence of any additive. Product 3 seems similar to the Control, since orange precipitate can be observed in all tested concentrations. Product 1 shows promising behavior at the highest tested concentration while products 2 and 4 perform as excellent dispersants even at lower concentrations. This becomes evident from the fact that, despite the yellow appearance of the solutions that indicate Stibnite presence, the solutions are clear, and no turbidity or precipitation is observed.

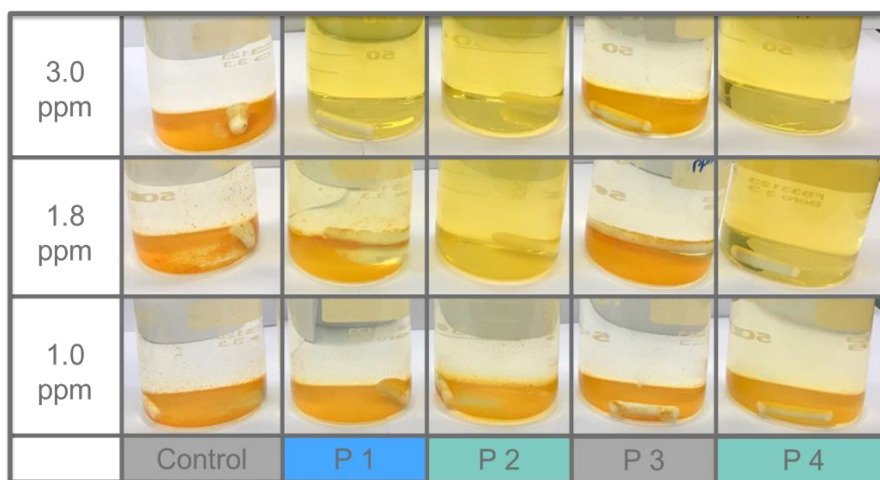


**Figure 6: Laboratory results of different products tested as Stibnite dispersants.**

While the most important first step through the journey of an inhibitor is the laboratory performance evaluation, it is as well crucial to confirm the positive results in the challenging conditions of the geothermal field. The trial reported in this work took place in Turkey, in an ORC plant. Initially, the deposit sample from the field was characterized with analytic techniques such as Scanning Electron Microscopy (SEM) and Electron Dispersive Spectroscopy (EDS) (see Figure 7).



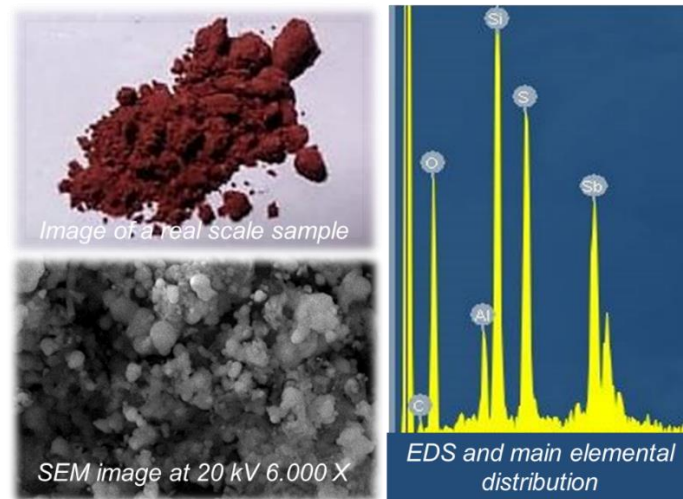


**Figure 7: Scale characterization of scaling occurred in a geothermal plant.**

From these acquired data it was concluded that a mixed scaling had to be mitigated, probably consisting of Aluminum silicate in addition to Stibnite. Therefore, the applied concept included the use of Kuritherm™ 4447, as an efficient stibnite inhibitor, mixed with silicate inhibitors in order to supply the optimum protection to the plant. As a control parameter additional to the installed coupons, the differential pressure in heat exchangers was carefully monitored (see Figure 8). The increase of this value is a direct indication of deposit formation. It was reported that minimal increase in differential pressure still occurs even after the initiation of the plant's treatment with the aforementioned product. However, the operation was able to remain clean and stable for a significant amount of time, with the need for a mechanical cleaning occurring only a year after said initiation.

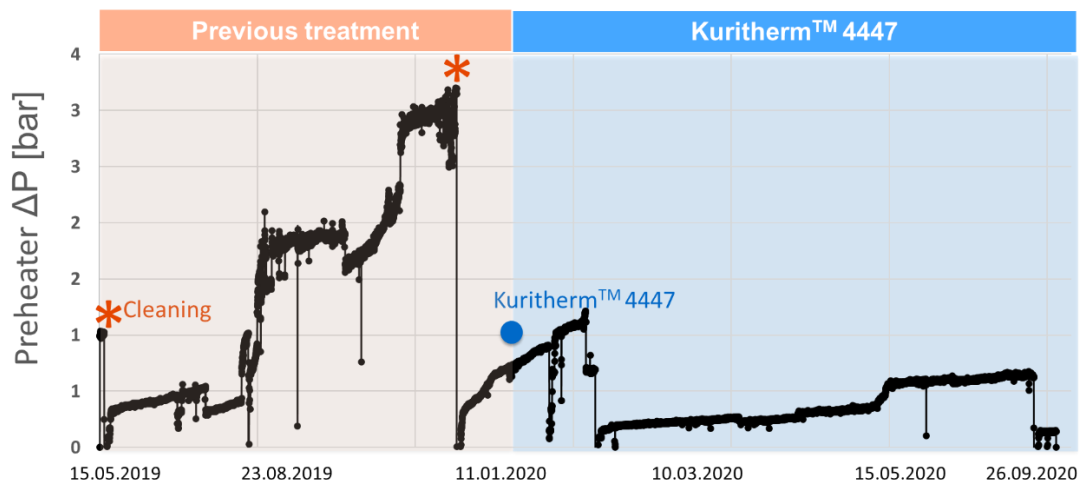


**Figure 8: Field Trial in an ORC plant in Turkey.**

#### 4. CONCLUSIONS

Two metal sulfides were investigated in terms of scale characteristics and idiosyncrasies: lead and antimony (III) sulfide. The test methods presented showed that chemical additives that pose as potential candidates for scale stabilization can prevent or delay the formation and / or settlement of lead sulfide and stibnite particles.



Regarding lead sulfide multiple test methods are shown and it is seen that particle size and settling speed varies based on the stirring time. Results produced with the turbidity meter suggest that a phosphonate-based inhibitor performs best when precipitation has already started but is less effective with regards to complete prevention of precipitations. So far indicative results reveal that scale prevention is rather achieved by substances based on phosphonates while dispersion is the domain of polycarboxylates. This reflects findings typically encountered upon calcite inhibition in the field of cooling water treatment. For antimony (III) sulfide a practical beaker test for dispersion effect of different inhibitors produced trustworthy results even at very low inhibitor concentrations and the results were evaluated visually. The successful candidates of these tests were implemented and tested in a real-life geothermal ORC plant in Turkey, where the efficiency was confirmed. A successful inhibitor like the product presented through this work can be translated in a variety of savings, such as reduction in the number of cleanings are necessary, which in its turn would mean savings in time and energy and gaining productive working hours of the plant.

## 5. LITERATURE

- Andritsos, N., Karabelas, A.J., 1991a. Crystallization and deposit formation of lead sulfide from aqueous solutions I. Deposition rates. *J. Colloid Interface Sci.* 145, 158–169.
- Andritsos, N., Karabelas, A.J., 1991b. Crystallization and deposit formation of lead sulfide from aqueous solutions II. Morphology of deposits. *J. Colloid Interface Sci.* 145, 170–181.
- Andritsos, N., Karabelas, A., 1995. An experimental study of sulfide scale formation in pipes. In: *Proceedings of the World Geothermal Congress, International Geothermal Association. Florence, Italy, 18-31 May 1995*, pp. 2469–2474.
- Bucher, K., Stober, I., 2010. Fluids in the upper continental crust. *Geofluids* 10, 241–253.
- Filella, M.; Belzile, N.; Chen, Y. Antimony in the environment: a review focused on natural waters: I. Occurrence, *Earth Sci. Rev.* 2002, 57, 125–176.
- Gallup, D.L., 1998a. Geochemistry of geothermal fluids and well scales, and potential for mineral recovery. *Ore Geol. Rev.* 12, 225–236.
- Gill, J.S.; Muller, L.; Rodman, D. Inhibition of Antimony Sulfide (Stibnite) Scale in Geothermal Fields, *GRC Transactions* 2013, 37.
- Helz, G.R.; Capps, N.E.; Valerio, M. Antimony Speciation in Alkaline Sulfide Solutions: Role of Zerovalent Sulfur, *Env. Science Technology* 2002, 36, 943-8.
- Shortall, R., Uihlein, A., 2019. Geothermal Energy and Technology Development Report 2018. EUR 29917 EN, European Commission, Luxembourg. <https://doi.org/10.2760/303626>. ISBN 978-92-76-12543-3.
- Smith, R.M., Martel, A.E., 1976. *Critical Stability Constants, Volume 4: Inorganic Complexes*. Springer Science and Business Media LLC, p. 77.
- White, D.E., 1981. Active geothermal systems and hydrothermal ore deposits. In: Skinner, B.J. (Ed.), *Seventy-Fifth Anniversary Volume; Economic Geology*. Publishing Company, pp. 392–423. <https://doi.org/10.5382/AV75>
- Wilson N.; Webster-Brown, J.; Brown, K. Controls on stibnite precipitation at two New Zealand geothermal power stations, *Geothermics*, 2007, 36, 330-347.